Phase diagram of high-T_c cuprates: Stripes, pseudogap, and effective dimensionality

V. V. Moshchalkov, J. Vanacken, and L. Trappeniers
Laboratorium voor Vaste-Stoffysica en Magnetisme, Katholieke Universiteit Leuven, Celestijnenelaan 200 D, B-3001 Heverlee, Belgium
(Received 28 July 2000; revised manuscript received 30 April 2001; published 1 November 2001)

The key problem in the physics of high T_c cuprates [J. G. Bednorz and K. A. Müller, Z. Phys. B **64**, 188 (1988)] is whether doping is inhomogeneous and holes are expelled into one-dimensional (1D) stripes. We demonstrate that the scattering mechanism defining the transport properties and the universal superlinear $\rho(T)$ behavior in underdoped $YBa_2Cu_3O_x$ thin films [J. Vanacken, Physica B **294–295**, 347 (2001)] is the same in spin ladders and underdoped cuprates. This implies that transport through conducting charge stripes in cuprates is fully controlled by the inelastic length coinciding with the magnetic correlation length in the ladders, i.e., holes in stripes behave very similarly to holes in spin ladders. The 1D stripe transport model describes remarkably well the temperature dependences of the resistivity and the scaling behavior of magnetic and transport properties of underdoped cuprates (including transport in fields up to 50 T) using essentially one fitting parameter—the spin gap—decreasing with hole doping. In the framework of this model the hole-rich stripes are just spin ladders with an even number of chains, and therefore the pseudogap is simply the spin gap in spin ladders. The effective dimensionality is 2D at high temperature and 1D in the pseudogap stripe regime. Disorder can lead to a pinning of stripes and their fragmentation, thus enforcing the interstripe hopping which effectively recovers the 2D transport regime at low temperatures.

DOI: 10.1103/PhysRevB.64.214504 PACS number(s): 74.25.Fy, 74.20.Mn, 75.10.Jm

I. INTRODUCTION

An undoped CuO_2 plane in cuprates can be considered as an insulating antiferromagnet.[1,2] Doping the planes with holes, leads to a variety of phenomena: suppression of the long-range antiferromagnetic (AF) order, an increase of conductivity resulting in an insulator-metal transition, the onset of the hole concentration (p)-dependent superconductivity, a transition from the insulating tetragonal to the metallic orthogonal structure, etc. The evolution of transport properties of high-T_c cuprates is extremely sensitive to the underlying microscopic magnetic structure,[3–8] and specific to the charge distribution in the CuO_2 planes. There is also growing experimental and theoretical evidence that the CuO_2 planes are not doped homogeneously, but instead, hole-rich one-dimensional (1D) features (''stripes'') are formed. In order to account for the possible inhomogeneous intercalation of AF insulating regions and metallic hole-rich stripes, a 1D stripe transport model was recently developed.[4] This model describes transport in the 1D striped regime, which becomes applicable below a certain temperature T^* where the pseudogap develops.[9] Rapidly growing experimental evidence[10–12] indicates that this 1D scenario might also be relevant for the description of the transport properties of the underdoped high-T_c cuprates. Since mobile carriers in this case are expected to be expelled from the surrounding Mott-insulator phase into the stripes, the latter then provide the lowest resistance paths. This makes the transport properties very sensitive to the formation of stripes, both static and dynamic. From this point of view, *a systematic study of the transport properties provides a unique possibility to probe the evolution of conducting stripes with the hole doping*. The main focus of the present paper is to demonstrate the applicability of the 1D stripe model to a description of the remarkable universal scaling behavior of the transport properties of the underdoped cuprates. We begin with a brief description of the model, and then test it on a well-defined case: transport in spin ladders (Sec. II). After that we use the very close similarity of the temperature dependence of the resistivity in two (seemingly different) compounds—spin ladders and underdoped cuprates. We argue that the 1D stripe model works very well for the underdoped cuprates (Sec. III). In the framework of this model, the temperature dependences of the resistivity and the Knight shift give the same spin gap value Δ. The doping dependence of Δ is discussed in Sec. III. The effects of disorder on the 1D stripes are presented in Sec. IV. Finally, the $T(p)$ phase diagram is discussed in terms of the stripe formation and effective dimensionalities (Sec. V).

II. DEVELOPMENT OF THE QUANTUM TRANSPORT MODEL IN DOPED 1D AND 2D HEISENBERG SYSTEMS

Figure 1 presents the scaled resistivity $(\rho-\rho_0)/(\rho_\Delta-\rho_0)$ versus the scaled temperature T/Δ [ρ_0 is the residual resistivity and $\rho_\Delta=\rho(T=\Delta)$]. This figure will act as a starting point for our discussion of the three different $\rho(T)$ regimes which we define as follows: linear behavior (I) $T>T^*$, superlinear behavior (II) $T_{MI}<T<T^*$, and ''insulating'' behavior (III), $T<T_{MI}$ with resistivity increasing at $T\rightarrow 0$. It is important to note here that we can interpret $\rho(T)$ curves in regime I in terms of a model of quantum transport in doped 2D Heisenberg systems.[3] Regime II can be related to the quantum transport in the 1D stripe phase.[4,5,13]

The CuO_2 planes in high-T_c cuprates play a crucial role in the determination of the transport properties. The confinement of the charge carriers in these planes reduces the dimensionality for charge transport to two dimensions or even to one dimension if stripes are formed. Depending on the effective dimensionality (2D or 1D), the transport properties will change accordingly. In both cases, however, it is reason-

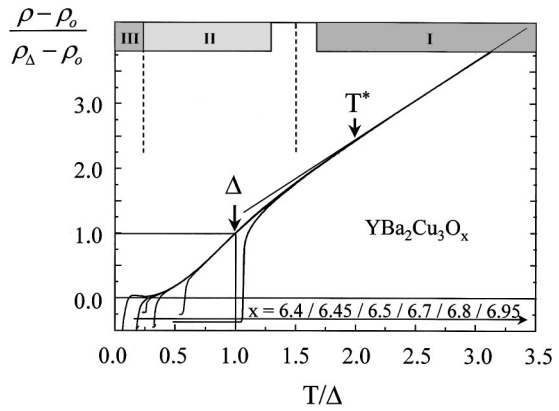

FIG. 1. Scaled zero-field resistivity data $\rho(T)$ for the $YBa_2Cu_3O_x$ films (from $x=6.4$ to $x=6.95$). The regions of different $\rho(T)$ behavior are indicated, as well as the energy scale Δ and the crossover temperature $T^*\approx 2\Delta$; ρ_0 is the residual resistivity, and ρ_Δ is the resistivity at $T=\Delta$.

able to expect that the following three basic assumptions can be fulfilled.[3,4]

(1) The dominant scattering mechanism in HTS in the whole temperature range is of *magnetic origin*;

(2) The specific temperature dependence of the resistivity $\rho(T)$ can be described by the inverse quantum conductivity σ^{-1} with the inelastic length L_ϕ being fully controlled, (via a strong interaction of holes with Cu^{2+} spins[14,15]) by the magnetic correlation length ξ_m, $L_\phi \sim \xi_m$.

(3) The proper 1D or 2D expressions should be used for calculating the quantum conductivity.

The 2D quantum conductivity is proportional to $\ln(L_\phi)$ whereas the quantum conductivity of a single 1D wire is a linear function of the inelastic length L_ϕ,[16]

$$\rho_{2D}^{-1}(T)=\sigma_{2D}(T)\sim \frac{1}{b}\frac{e^2}{\hbar}\ln(L_\phi/l), \tag{1}$$

$$\rho_{1D}^{-1}(T)=\sigma_{1D}(T)\sim \frac{1}{b^2}\frac{e^2}{\hbar}L_\phi, \tag{2}$$

with l the elastic length and b the thickness of the 2D layer or the diameter of the 1D wire. These expressions for the resistivity of the 2D layers and 1D wires can be used further on to calculate $\rho(T)$ by simply inserting into the elastic length $L_\phi \sim \xi_m$ (ξ_m being the magnetic correlation length) into Eqs. (1) and (2). The determination of the precise behavior of the resistivity in the 2D Heisenberg ($T>T^*$) and the 1D striped ($T<T^*$) regimes thus requires a knowledge of the magnetic correlation lengths in 2D(ξ_{m2D}) and 1D(ξ_{m1D}) cases.

In the framework of the 2D Heisenberg model, which is certainly applicable for the doped CuO_2 planes without any stripes present, the temperature dependence of the correlation length ξ_{m2D} is expressed as[17]

$$\xi_{m2D}(T)=\frac{e\hbar c}{8\times 2\pi F^2}\left(1-\frac{T}{2\times 2\pi F^2}\right)\exp\left(\frac{2\pi F^2}{T}\right) \tag{3}$$

with c being the spin velocity and F a parameter that can be directly related to the exchange interaction J, where $2\pi F^2 = J$. Equation (3) was derived for *undoped* 2D Heisenberg systems. Numerical Monte Carlo simulations,[18] however, also demonstrated its validity for weakly doped systems.

For the 1D striped phase, the striking similarity of $\rho(T)$ curves in underdoped cuprates and spin ladders (see below) implies that the 1D even-chain Heisenberg AF spin-ladder model can be employed to describe the $\rho(T)$ of the striped phase. The 1D spin-correlation length ξ_{m1D} found for the undoped ladders by Monte Carlo simulations[19] is given by

$$(\Delta\xi_{m1D})^{-1}=\frac{2}{\pi}+A\left(\frac{T}{\Delta}\right)\exp\left(\frac{-\Delta}{T}\right), \tag{4}$$

where $A\approx 1.7$ and Δ is the spin gap. We assume here that Eq. (4) can still be applied for weakly doped ladders as well.

The next natural step is the combination of these expressions for the 1D and 2D spin correlation lengths with the proper expressions for the quantum resistance, which eventually gives expressions for the temperature dependence of the resistivity. In the 2D Heisenberg regime, remarkably, the resistivity is a linear function of temperature[3] due to the mutual cancellation in the limit $T\ll 2J$ of the logarithmic $\rho(\xi_m)$ dependence and the exponential temperature dependence of ξ_m. Therefore, the linear ρ versus T universal behavior at $T>T^*$ can be related to the doped 2D Heisenberg systems regime:

$$\rho_{2D}(T)=[\sigma_{2D}(T)]^{-1}\sim[\ln(\xi_m)]^{-1}\sim\left[\ln\left(\exp\left(\frac{J}{T}\right)\right)\right]^{-1}\sim\frac{b\hbar T}{e^2 J}. \tag{5}$$

The 1D spin-ladder resistivity can be described by Eq. (6), with $J_\parallel$ the intrachain coupling and a the spacing between the 1D wires ($J_\parallel$ comes in to recalculate the theorist units):[4,6]

$$\rho_{1D}(T)=[\sigma_{1D}(T)]^{-1}=\frac{\hbar b^2}{e^2 a}\left\{\frac{2\Delta}{\pi J_\parallel}+A\frac{T}{J_\parallel}\exp\left(-\frac{\Delta}{T}\right)\right\}. \tag{6}$$

Note that this expression is *not* an empirical interpolation formula. On the contrary, this expression is derived for transport in the spin ladders, and therefore it combines important microscopic parameters (Δ and $J_\parallel$) describing the spin-gap and exchange interaction in the spin ladders.

To verify the validity of the proposed model of the quantum transport in the 1D spin ladder model, a crucial test is its application to the resistivity data obtained on the well-known even-chain spin-ladder compound $Sr_{2.5}Ca_{11.5}Cu_{24}O_{41}$.[20] This compound, due to its specific crystalline structure, definitely contains a two-leg ($n_c=2$) Cu_2O_3 ladder, and therefore its resistivity along the ladder direction should indeed obey the 1D conductivity expression given by Eq. (6). The results of the $\rho(T)$ fit with Eq. (6) are shown in Fig. 2(a). This fit demonstrates a very good quality over the temperature range $T\sim 25-300$ K, except for the lowest temperatures where the onset of the localization effects, not taken into account in Eq.

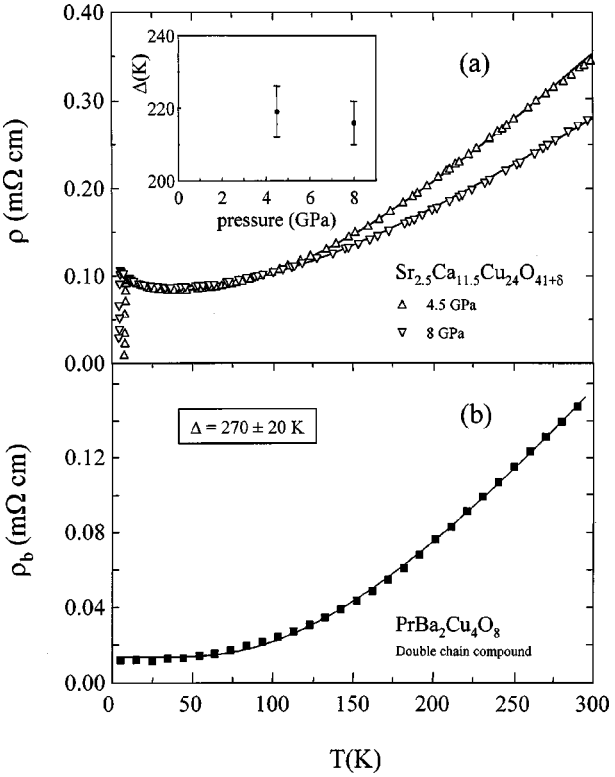

FIG. 2. (a) Temperature dependence of the resistivity for a $Sr_{2.5}Ca_{11.5}Cu_{24}O_{41}$ even-chain spin-ladder single crystal at 4.5 and 8 GPa (experimental data points after Ref. 20). The solid line represents a fit using Eq. (6) describing transport in 1D SL's. (b) Temperature dependence of the *b*-axis resistivity of $PrBa_2Cu_4O_8$ (Ref. 22) together with a fit using Eq. (6).

(6), is clearly visible in the experiment. Moreover, the fitting parameters ρ_0, C, and Δ all show very reasonable values.

The expected residual resistance for $b\sim 2a\sim 7.6$ Å, $\Delta\sim 200$ K, and $J_{\parallel}\sim 1400$ K (the normal value for the CuO_2 planes) is $\rho_0\sim 0.5\times 10^{-4}\,\Omega$ cm, which is in good agreement with $\rho_0\sim 0.83\times 10^{-4}\,\Omega$ cm found from the fit. The fitted gap $\Delta\sim 216$ K (at 8 GPa) [Fig. 2(a)] is close to $\Delta\sim 320$ K determined for the undoped superlattice (SL) $SrCu_2O_3$ from inelastic neutron scattering experiments.[21] In doped systems it is natural to expect a reduction of the spin gap upon doping. Therefore, the difference between the fitted value (216 K) and the one measured in an undoped system (320 K) seems to be quite fair. Finally the calculated fitting parameter $C=(A\pi\rho_0)/2\Delta=0.0103$ (in units of $10^{-4}\,\Omega$ cm K) is to be compared with $C=0.013$ [from the 8-GPa fit in Fig. 2(a)]. Using the fitting procedure for the two pressures 4.5 GPa ($\Delta\sim 219$ K) and 8 GPa ($\Delta\sim 216$ K), we have obtained a weak suppression of the spin-gap under pressure $d\Delta/dp\sim -1$ K/GPa.

Another model system to check the validity of the 1D transport model[4] is the $PrBa_2Cu_4O_8$ compound. This compound has a well-known double Cu-O chain. The results of the high-pressure studies of this Pr124 material suggest that the metallic conduction here is governed by the double Cu-O chains, and not by the CuO_2 plane.[22] The metallic behavior along the Cu-O chain in Pr124 deserves a special attention

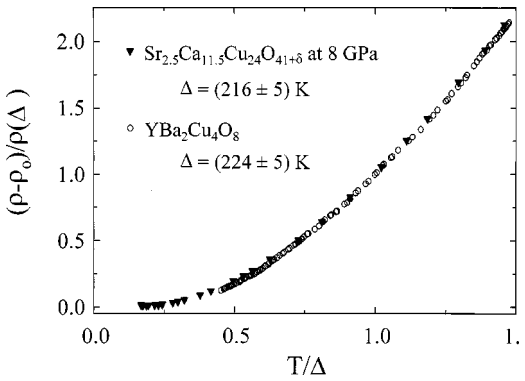

FIG. 3. Scaling analysis on the temperature dependence of the resistivity of the underdoped high-T_c superconductor $YBa_2Cu_4O_8$ and the even-leg spin-ladder $Sr_{2.5}Ca_{11.5}Cu_{24}O_{41}$.

because it can provide a unique and interesting opportunity to study the 1D two-leg ladders. As can be concluded from a fit using Eq. (6), the 1D expression for the resistivity works rather well for this double chain compound. Both the fit and the experimental data[22] are shown in Fig. 2(b).

The next crucial step in our analysis is the comparison of the $\rho(T)$ curves in the spin ladders and underdoped high-T_c cuprates. Interestingly, both compounds, seemingly belonging to different dimensional regimes, show practically the same temperature dependence of the scaled resistivity (Fig. 3).

The superlinear $\rho(T)$ behavior observed in the doped even-chain SL under external pressure indicates, by its similarity with the S-shaped $\rho(T)$ in underdoped HTS, that the picture of 1D transport might be relevant to the HTS at $T<T^*$, where a superlinear $\rho(T)$ behavior is clearly seen (Figs 1–3). To investigate the possibility of using the 1D scenario for describing transport properties of the 2D CuO_2 planes of the high-T_c superconductors, it is appropriate to compare the temperature dependence of the resistivity of a typical underdoped high-T_c material $YBa_2Cu_4O_8$ with that of the even-chain SL compound $Sr_{2.5}Ca_{11.5}Cu_{24}O_{41}$.

The crystal structure of the $YBa_2Cu_4O_8$ compound (''124'') differs substantially from that of the more common $YBa_2Cu_3O_7$ (''123''), since 124 contains double CuO chains stacked along the *c*-axis and shifted by *b*/2 along the *b* axis.[23] These chains are believed to act as charge reservoirs; therefore, they may have a strong influence on the transport in the CuO_2 planes themselves. In the 124 case, the 1D features of this double CuO chain can be expected to induce an intrinsic doping inhomogeneity in the neighboring CuO_2 planes, thus enhancing the formation of 1D stripes in the planes in a natural way. A weak coupling of the 1D chains to the 2D planes might be sufficient to reduce the effective dimensionality by preferentially orienting the stripes in the CuO_2 planes along the chains. But even in pure 2D planes, without coupling to the 1D structural elements the formation of the 1D stripes is possible. Using a simple scaling parameter Δ, a perfect overlap of the two sets of data was found: $(\rho-\rho_0)/\rho(\Delta)$ versus T/Δ (with ρ_0 being the residual resistance) for $YBa_2Cu_4O_8$ and $Sr_{2.5}Ca_{11.5}Cu_{24}O_{41}$ (Fig. 3). Note that ρ_0 should be subtracted from $\rho(T)$ since ρ_0, depending

on the sample quality, may contain contributions from several additional scattering mechanisms.

This perfect scaling of the $\rho(T)$ data of an underdoped HTS on one side and an even-leg spin ladder on the other side has very important implications for the understanding of the nature of the charge transport and the scattering in the high-T_c cuprates' CuO_2 layers. It convincingly demonstrates that *resistivity vs temperature dependence of underdoped cuprates in the pseudogap regime at $T<T^*$ and even-chain SL with a spin-gap Δ are governed by the same underlying 1D (magnetic) scattering mechanism.*

Early experiments on twinned high-T_c samples however, created an illusion that all planar Cu sites in the CuO_2 planes are equivalent. Recent experiments on perfect untwinned single crystals have strongly questioned this belief. A very large anisotropy in the *ab* plane of twin-free samples was reported for resistivity $[\rho_a/\rho_b(YBa_2Cu_3O_7)=2.2$ (Refs. 24 and 25) and $\rho_a/\rho_b(YBa_2Cu_4O_8)=3.0$ (Ref. 26)], thermal conductivity $[\kappa_a/\kappa_b(YBa_2Cu_4O_8)=3-4$ (Ref. 27)] superfluid density,[28,29] and optical conductivity.[29,30] In all these experiments, much better metallic properties have been clearly seen along the direction of the chains (the *b* axis). And what is truly remarkable, that this in-plane anisotropy can be partly suppressed by a vary small (only 0.4%) amount of Zn,[29] which is known to replace copper, at least for Zn concentrations up to 4%, only in the CuO_2 planes.[31,32] The latter suggests that the *ab* anisotropy cannot only be explained just by assuming the existence of highly conducting CuO chains. Instead, the observation of anisotropy in the transport properties in the *ab* plane for $YBa_2Cu_4O_8$ (Ref. 26) and $YBa_2Cu_3O_7$,[24] interpreted as a large contribution of strongly metallic Cu-O chains $\rho_{\rm chain}(T)$, might be reinterpreted taking into account the fact that the in-plane anisotropy is caused by certain processes in the CuO_2 planes themselves, where the substitution of Cu by Zn takes place. In this situation we may expect that the chains are actually imposing certain preferential directions in the CuO_2 planes for the formation of 1D stripes.

However, inelastic neutron-scattering experiments on $YBa_2Cu_3O_7$ (Refs. 33–35) show evidence of the existence of rather dynamic stripes, and the observation of 1D features in the transport properties should therefore not be limited to the Cu-O chain-direction only. Moreover, although the 1D stripes are dynamic, no averaging of the transport properties will occur, since, even for dynamic stripes, the charge will automatically follow the most conducive paths, i.e., stripes, even if they are moving fast. Fitting the 1D quantum transport model[4] to the inplane $\rho(T)$ curve for $YBa_2Cu_4O_8$ [Eq. (6)] results in a very nice fit,[4–8] yielding a spin gap $\Delta=224\pm5$ K (Figs. 3 and 4). The slope of $\ln[(\rho-\rho_0)/T]$ versus $1/T$ (see the inset in Fig. 4) defines the spin-gap value, thus reducing the number of the fitting parameters in this case to only one: ρ_0. Therefore, we can conclude that the resistivity of underdoped cuprates below T^* (see the inset in Fig. 4) simply reflects the temperature dependence of the magnetic correlation length *in the even-chain SL's, associated with stripes and the pseudo-gap is the spin-gap formed in the 1D stripes*.

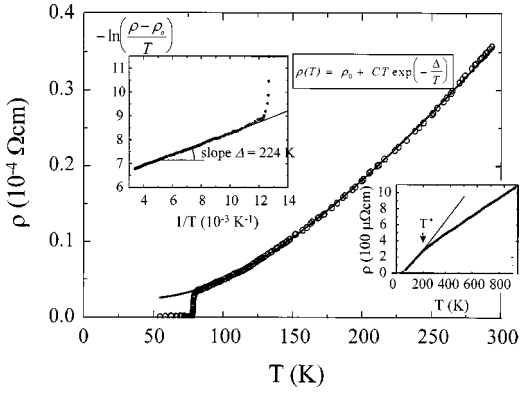

FIG. 4. Temperature dependence of the resistivity of a $YBa_2Cu_4O_8$ single crystal (open circles); the solid line represents the fit using Eq. (6). The fit parameters are $\rho_0=0.024\times10^{-4}\,\Omega$ cm, $C=0.00242\times10^{-4}\,\Omega$ cm/K, and $\Delta=224$ K. The high-temperature data taken on another crystal (Ref. 36) shown in the inset, illustrate the 1D-2D crossover (linear behavior) at $T>T^*$. Insert (upper left): the determination of the spin gap Δ from the special plot based on Eq. (6). This plot gives the spin gap, using only one fitting parameter (ρ_0).

In order to substantiate these observations, we can use similar ideas in the analysis of other physical properties. Since in underdoped cuprates the spin-gap temperature Δ found from the $\rho(T)$ scaling works equally well for resistivity as for Knight-shift data K_S,[38] these K_S data can also be used for fitting with the expressions derived from the 1D SL models. For a two-leg SL, the temperature dependence of the Knight shift K_S is.[37]

$$K_S(T)\sim T^{-1/2}\exp(-\Delta/T) \tag{7}$$

Fitting the $K_S(T)$ data[37] for $YBa_2Cu_4O_8$ with this expression gives an excellent result (Fig. 5) with a spin gap $\Delta=222\pm20$ K, which is very close to the value $\Delta=224\pm5$ K derived from the resistivity data.

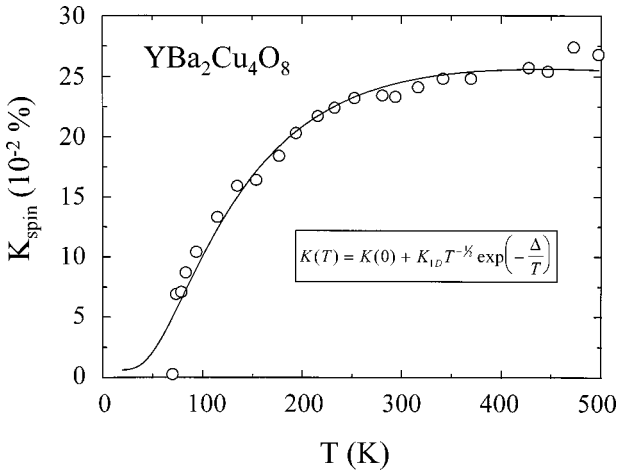

FIG. 5. Knight-shift data $K_S(T)$ for the $YBa_2Cu_4O_8$ system (Ref. 36) fitted with Eq. (7) (see also the inset) for two-leg spin ladders (Ref. 37). The resulting fitting parameters are $K(0)=(0.6\pm2)\times10^{-2}\%$, $K_{1D}=(870\pm40)\times10^{-2}\%$, and $\Delta=(222\pm20)$ K (Refs. 7 and 8).

Therefore, for an underdoped HTS, we have related the linear $\rho(T)$ behavior above T^* with quantum transport in a 2D AF Heisenberg system and the S-shaped superlinear behavior below T^* with a 1D quantum transport model for even-chain spin ladders (the striped phase). In the next sections we will interpret the universal $\rho(T)$ behavior in the framework of this 1D-2D model, extract the spin gap Δ, and discuss the experimental $T(p)$ phase diagram.

III. DOPING DEPENDENCE OF THE SPIN GAP IN $YBa_2Cu_3O_x$

As can be seen from Fig. 1, the in-plane resistivity $\rho_{ab}(T)$ of underdoped $YBa_2Cu_3O_x$ shows a linear $\rho(T)$ dependence at high temperatures $T>T^*$, a superlinear behavior at $T<T^*$, and an increasing resistivity at the lowest temperatures for strongly underdoped samples. This insulating-like $\rho(T)$ behavior was revealed by the application of very high magnetic fields in order to suppress superconductivity.[39] Doping the high-T_c materials reduces the tendency toward insulating behavior, and lowers the crossover temperature T^* so that the superlinear $\rho_{ab}(T)$ gives way for the linear region, which is expanding to lower temperatures. These in-plane resistivities are shown to scale onto one universal curve (Fig. 1). From this plot, a perfect scaling in regimes I (linear part) and II [curved, superlinear $\rho(T)$] was observed for all the zero-field curves. In the insulating regime (III), the scaling is of less good quality. The perfect scaling of the metallic in-plane resistivities for these compounds is a strong indication that one scattering mechanism is dominant for the strongly underdoped samples up to the near optimally doped samples. Only the energy scale (the scaling parameter Δ and the crossover temperature $T^*\approx 2\Delta$) varies with doping. Based on the analysis given in the previous paragraph, it is reasonable to try to correlate this ''dominant process'' with the magnetic scattering mechanisms in one and two dimensions, introduced there.

For $T>T^*$, where short-range AF fluctuations are seen in inelastic neutron scattering experiments, the resistivity is found to have a linear temperature dependency (region I). This regime is thus described by Eq. (5) for quantum transport in a 2D Heisenberg system with the inelastic length determined by the magnetic (2D) correlation length.[13]

For temperatures below $T<T^*\approx 2\Delta$, 1D stripes are formed, thus reducing the effective dimensionality from 2D to 1D, and the spin gap Δ is clearly seen in the S-shaped universal scaled $\rho(T)$ (regime II). This regime should then be accurately described by Eq. (6), corresponding to quantum transport in a 1D striped material with again the inelastic length being determined by the magnetic (1D) correlation length. To check this, the $\rho(T)$ curve shown in Fig. 1 describes both these expressions [Eqs. (5) and (6)] and the experimental data. A perfect overlap with the data is established up to slightly above $T/\Delta=1$. The scaling of the data was performed such that the data fall onto the universal $\rho(T)=\rho_0+C\,T\exp(-\Delta/T)$ curve with $C=\exp(1)=2.718$. In that way, the scaling parameters necessary to obtain the collapsing $\rho_{ab}(T)$ traces directly yield estimates for the spin pseudo-gap Δ within this model for transport in a 1D striped case.

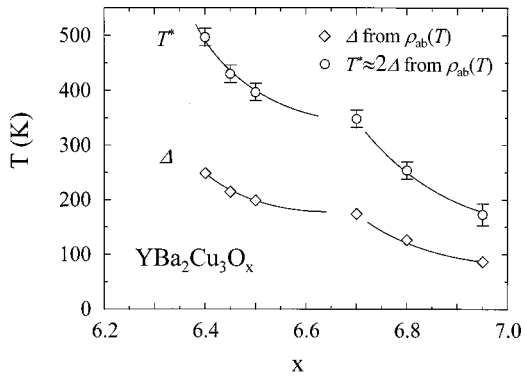

FIG. 6. Spin gap Δ and crossover temperature $T^*\approx 2\Delta$ for the $YBa_2Cu_3O_x$ thin films, as derived from the scaling of their in-plane resistivities $\rho_{ab}(T)$ with the curve for 1D quantum transport.

In Fig. 6, the estimates for the spin pseudogap Δ and the crossover temperature $T^*\approx 2\Delta$ are, for the $YBa_2Cu_3O_x$ system,[2] plotted versus the oxygen content x. Like T^*, the spin-gap decreases upon doping, approaching the critical temperature T_c near the optimally doped case. This is a well-documented trend for the pseudogap, and is not restricted to the $YBa_2Cu_3O_x$ compounds (for a review, see Ref. 40).

A crucial check for the 1D conductivity model[4] is the direct comparison of our values for the pseudogap with estimates from the literature. In Fig. 7, we replot our $\Delta(x)$ data on thin films (open diamonds) together with estimates from resistive measurements on other $YBa_2Cu_3O_x$ thin films,[38] and on twinned[41] and detwinned[27] single crystals. Within the error bars, these data agree well. Additionally, we have plotted estimates of the pseudogap as derived from the CuO_2 plane ^{17}O and ^{63}Cu Knight-shift measurements on aligned powders.[42,43] Also these data, although obtained with a totally different technique, resulted in spin-gap values that are

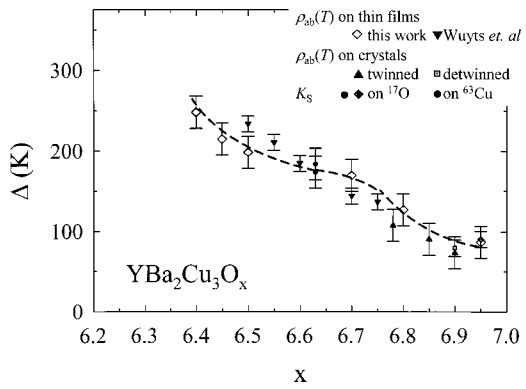

FIG. 7. The spin gap Δ of $YBa_2Cu_3O_x$ vs oxygen content x, from the scaling of the $\rho_{ab}(T)$ data with the curve for the 1D quantum transport for the thin films in this work (open diamonds) and a direct fit on the films from Ref. 38 (down triangles), twinned crystals (Ref. 41) (up triangles) and detwinned crystals (Ref. 24) (squares). The spin gap obtained from a fit of the Knight shift on ^{17}O (Ref. 43) (filled diamonds) and on ^{63}Cu and ^{17}O (Ref. 42) (circles) is also added.

in good agreement with our $\Delta(x)$ data. This proves that the 1D quantum transport model,[4] used to describe the transport in underdoped cuprates at $T<T^*$,[5,6] not only agrees qualitatively, but also yields very reasonable values for the pseudo spin-gap Δ that agree well with other independent data.

Although this correspondence is quite convincing, it should be mentioned that experimental techniques probing charge excitations (like angle-resolved photoemission spectroscopy, quasiparticle relaxation measurements, and tunneling experiments) give pseudogap Δ_p values that are significantly higher (about a factor 2) than the spin-excitation gap Δ_s, as observed in NMR and INS experiments.[40,44] In the 1D quantum transport model, where the inelastic length is assumed to be dominated by the magnetic correlation length, the agreement of our data with the gap-value determined from NMR experiments then seems to be natural.

The only difference in this discussion comes from the often-cited ^{89}Y NMR data on underdoped $YBa_2Cu_3O_x$ reported by Alloul and co-workers.[45] These Knight-shift data were shown earlier to scale very well, using the same scaling temperature T_0 that was derived from the scaling of $\rho_{ab}(T)$.[38] This was interpreted as a strong indication that the opening of the spin-gap seen in the Knight shift is relevant also for transport properties thus motivating the development of the 1D/2D quantum transport model.[4–6] This argument still holds. However, when fitting the expression for the Knight shift $K_S(T)$ (as in figure 5) to these data, the resulting values for the pseudo-gap are about a factor 2 higher than the gap values determined from resistivity measurements or the data on in-plane ^{17}O and ^{63}Cu Knight-shift on aligned powders.[42,43] The origin of this deviation is not clear but could be due to the use of non-aligned powders[45] or possible differences between NMR measurements probing inter-plane ^{89}Y or in-plane ^{17}O and ^{63}Cu.

If one looks at the $T^*(x)$ or $\Delta(x)$ experimental data, one can see that, as a function of oxygen content, around $x \sim 6.6$ a plateau arises in both curves, just like in the $T_c(x)$ curve. Therefore, there seems to be a common concentration dependency for both the opening of the spin gap, and for the occurrence of superconductivity.

IV. DISORDER-INDUCED STRIPE PINNING AND FRAGMENTATION AT LOW TEMPERATURES

At low temperatures, $T<T_{\mathrm{MI}}$, the metallic behavior of the resistivity in regions I and II transforms into an insulating, diverging, $\rho(T)$ (region III).[2,39] The diverging high-field $\rho(T)$ data were shown to agree better with the $\ln(1/T)$ divergence than with a simple power law $T^{-\alpha}$.[46] Although the origin of such a logarithmic divergence is still strongly debated, it is interesting to analyze our data for the normal-state resistivity within the framework of the model considering stripe formation in the CuO_2 plane.

In the charge-stripe picture,[6,7,12,14,35,47] dynamic metallic[30,48,49] stripes are thought to dominate the transport properties. So, within this model, one expects a strong influence on the transport properties when, for some reasons, the 1D charge stripes are fragmented and/or pinned. In the presence of stripe fragmentation, charge carriers are forced to hop to neighboring metallic stripes or their fragments passing through the intercalating Mott-insulator areas. This leads to an increased resistivity[49] (see Fig. 9 below). Interstripe hopping recovers effectively the 2D transport regime and then the low-temperature $\ln(1/T)$ increase of the high-field resistivity can be interpreted as weak localization effects, typical for the 2D case.

One possible type of pinning centers which might be responsible for stripe pinning and fragmentation is the crystallographic disorder in the CuO_2 plane, in the form of dislocations. These dislocations will also alter the local electronic and magnetic structure in the plane and at low temperatures, when the stripes are less mobile; they can be expected to pin the magnetic domain walls formed by the charge stripes. Moreover, in the case of strong pinning, stripe fragmentation is predicted to occur.[50]

Experimentally, the pinning of charge stripes has been seen by neutron-diffraction experiments on the Nd-doped and pure $La_{2-x}Sr_xCuO_4$.[12] The striking result derived from these data is that, although the incommensurate features (i.e., the stripes) are almost identical, the scattering in the pure, near optimally doped, $(La_{2-x}Sr_x)CuO_4$ system is inelastic (dynamic stripes) whereas in the $(La_{1.6-x}Nd_{0.4}Sr_x)CuO_4$ system elastic scattering is observed, corresponding to static stripes. In general, pinning of these stripes is correlated with the onset of an increasing resistivity,[48] although stripe pinning has been found in underdoped samples that are metallic (but close to the metal-insulator transition),[49] suggesting stripe fragmentation to be as important as pinning for the creation of an insulating state.

So, for dynamic stripes, the resistivity will be quasi-1D metallic and the Hall response in a magnetic field will remain finite, since dynamic charge stripes are still able to respond to the transverse electric field acting on the charge carriers. For pinned stripes that are not fragmented, the resistivity can be expected to remain essentially metallic since the 1D metallic wires remain unbroken. However, such a reduced mobility of the stripes can be expected to have a noticeable influence on the Hall effect. When the stripes are pinned, they cannot properly react to the Lorentz force acting on the charge carriers, and only a reduced Hall field (and thus Hall resistivity ρ_{xy}) is built up. However, in the presence of stripe fragmentation or interstripe hopping, also Hall effect will be present due to the charge interstripe hopping across the Mott-insulator phase. This will result in an insulating longitudinal resistivity and a small but finite Hall effect.

Recently, based on the Hall effect and x-ray measurements on Nd-doped $La_{2-x}Sr_xCuO_4$ crystals,[48] it was argued that the Hall conductivity σ_{xy} [Eq. (8)] could be related to the inverse stripe order:

$$\sigma_{xy}(H)=\frac{\rho_{yx}}{\rho_{xx}^2+\rho_{xy}^2}\approx\frac{\rho_{yx}}{\rho_{xx}^2}=\frac{R_H B_z}{\rho_{ab}^2}\approx\frac{R_H\mu_0 H}{\rho_{ab}^2(H)}. \qquad (8)$$

In order to check this idea, we have combined our high-field $\rho_{ab}(T)$ curves with the $R_H(T)$ data obtained on the same samples, above and below T_c to calculate the Hall conductivity σ_{xy} using Eq. (8). The results are summarized in

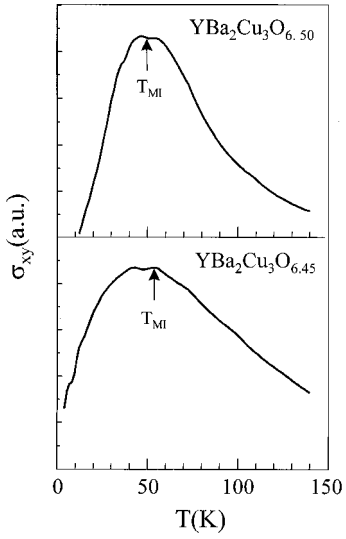

FIG. 8. The off-diagonal conductivity σ_{xy}, calculated by combining the Hall coefficient R_H and the in-plane resistivity ρ_{ab} at 40 Tesla [Eq. (8)]. The arrows indicate the temperature T_{MI} where the resistivity starts to increase with lowering temperature, and the x axis is drawn at $\sigma_{xy}=0$.

Fig. 8 for all the samples showing a pronounced divergence of the low-temperature resistivity.

From the plots in Fig. 8, it is clear that, once the resistivity starts increasing at low temperatures (at $T<T_{\mathrm{MI}}$), also the Hall conductivity goes down rapidly and hence, according to the analysis made in Ref. 48, stripe order in these underdoped $YBa_2Cu_3O_x$ and $Y_{0.6}Pr_{0.4}Ba_2Cu_3O_x$ samples increases. However, a significant difference from Ref. 48 must be pointed out: in our data, the decreasing Hall conductivity σ_{xy} is almost completely due to the strongly diverging longitudinal resistivity $\rho_{ab}(T)$, whereas the Hall response $R_H(T)$ remains finite (and approximately temperature independent) down to the lowest temperatures used in our experiments.

When combining this result with the discussion about dynamic versus static pinned stripes, it becomes clear that, at low temperatures, the charge stripe picture can only be brought into agreement with our normal state transport data by assuming stripe fragmentation or/and interstripe hopping effects. This causes an effective recovery of the 2D regime. By inserting the temperature dependence of the inelastic length L_ϕ, of the scattering mechanisms applicable for the intercalating insulating phase, into the conductivity expression for 2D quantum transport [Eq. (8)] one can calculate the low-temperature $\ln(1/T)$ divergence of the high-field resistivity. For example, the inelastic length for electron-electron or electron-phonon scattering, $L_\phi \sim 1/T^\alpha$,[16] combined with the 2D quantum transport, gives a $\ln(1/T)$ correction to the low-temperature resistivity. Also electron interference effects in the 2D weak-localization theory can be responsible for the $\ln(1/T)$ behavior. Moreover, this 2D weak-localization model also agrees with our finding of a constant Hall coefficient $R_H(T)$ at low temperatures.

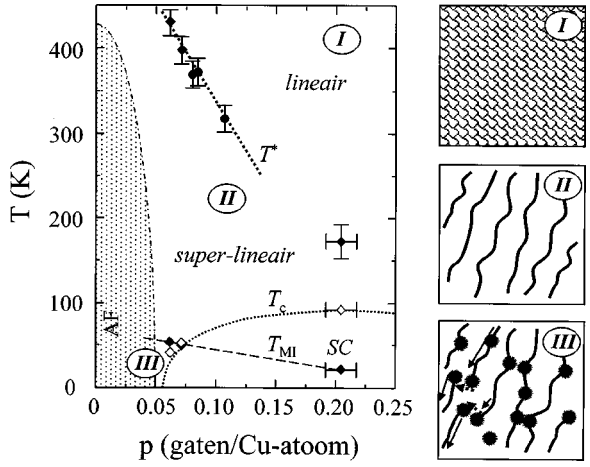

FIG. 9. The generic $T(p)$ phase diagram for the $YBa_2Cu_3O_x$ (diamonds, solid line) thin films. Indicated are the 2D-1D crossover temperature T^* (filled symbols), the superconducting critical temperature T_c (open symbols), and the boundary T_{MI} between the metallic and the insulating regimes for $\rho(T)$. All are plotted versus the fraction of holes per Cu atom in the CuO_2 plane. In regime (I) 2D quantum transport takes place; in regime II, 1D stripe transport dominates; finally, in region III, 2D transport is effectively recovered due to the interstripe hopping and stripe pinning.

V. $T(p)$ PHASE DIAGRAM: STRIPES DEFINE PSEUDOGAP AND EFFECTIVE DIMENSIONALITY

The construction of the $T(p)$ phase diagram, describing the superconducting and normal-state transport properties of the $YBa_2Cu_3O_x$ compounds, requires the combination of our high-field transport data and the estimates for the carrier concentration from the Hall effect. This experimental phase diagram can now be discussed in the framework of the 1D-2D quantum transport model[3–7] (Fig. 9). Of course, regardless of this interpretation, the experimental $T(p)$ phase diagram, including its crossover lines, remains valid. Three different regimes (I–III) are present in the $T(p)$ diagram. In Region I, a metallic linear temperature dependence of the resistivity is observed ($T>T^*$). It can be described by the expression for a 2D Heisenberg system where short-range AF fluctuations are revealed in inelastic neutron scattering experiments. In Region II, when an underdoped high-T_c cuprate is cooled below T^*, an S-shaped $\rho(T)$ develops, that can be scaled onto a single universal curve for the Y-Ba-Cu-O compounds. This curve is accurately described by the model for transport in a 1D striped regime (region II), and yields values for the spin gap that agree well with estimates found from the literature. *The stripes correspond to the doped spin ladders with an even number of legs*.[4] *From this point of view, the pseudogap is just the spin gap in the ladder compounds*. This gap decreases with an increase the hole concentration p. The 1D striped regime is defined by the four boundaries in the $T(p)$ diagram. At low doping levels, the bulk antiferromagnetic order is recovered and the stripes disappear. At high doping levels, the distance between stripes is expected to decrease; charges start to leak into the Mott insulator phase between the stripes and as a result, the charge stripes col-

lapse completely when $T_c \rightarrow 0$. At high temperatures, entropy effects and stripe meandering are expected to destroy the 1D regime, recovering the 2D regime with antiferromagnetic fluctuations. At low temperatures $T < T_{\mathrm{MI}}$, stripe pinning, fragmentation and interstripe hopping effects establish a 2D insulating regime (region III). In the $T(p)$ diagram, the onset of this insulating regime is indicated by T_{MI}, below which the resistivity increases with lowering temperature. *Depending on the disorder, the MI transition line at $T=0$ K can be shifted*. At low temperatures $T < T_c$, the onset of a macroscopic coherence between the so-called pre-formed pairs[14,15] is predicted to result in the recovery of the bulk superconductivity (in the absence of high magnetic fields).

VI. CONCLUSIONS

The universal $\rho(T)$ behavior in the underdoped $YBa_2Cu_3O_x$ thin films is a strong indication of one single scattering mechanism being dominant over the whole underdoped regime in the Y123 system. Only the energy scale (the scaling parameter Δ—the spin gap—and the crossover temperature $T^* \approx 2\Delta$) varies upon doping.

Any model trying to explain the extraordinary features of the normal-state transport properties of the high-T_c's [linear $\rho(T)$ at high temperatures, S-shaped $\rho(T)$ at intermediate temperatures and logarithmically diverging $\rho(T)$, etc.] should also account for the complex magnetic phase diagram for these high-T_c cuprates. In the underdoped region of this diagram, at moderate temperatures $T > T^*$, 2D antiferromagnetic correlations are present in the CuO_2 planes. Moreover, an increasing amount of experimental and theoretical observations is clearly in favor of the existence of dynamic one-dimensional charge stripes in the CuO_2 planes at $T < T^*$, acting as domain walls for the antiferromagnetic fluctuations. These local charge inhomogeneities (1D charge stripes) will confine the AF regions, resulting in the formation of a pseudo-spin-gap at temperatures far above the superconducting critical temperature T_c.

It is then tempting to assign the origin of the dominant scattering mechanism for charge transport to the microscopic magnetic correlations in the planes of the high-T_c cuprates. The importance of the CuO_2 planes for the transport properties is a widely documented feature of the high-T_c cuprates. The confinement of the charge carriers in these planes reduces the dimensionality for charge transport to two dimensions (or less when stripes are formed) and makes the conductivity σ in such 2D metallic system to be controlled by quantum transport. In this case the approach based on the following three basic assumptions can be used.[3,4] (i) The dominant scattering mechanism in HTS in the whole temperature range is of magnetic origin. (ii) The specific temperature dependence of the resistivity $\rho(T)$ can be described by the inverse quantum conductivity σ^{-1} with the inelastic length L_ϕ being fully controlled by the magnetic correlation length $\xi_m (L_\phi \sim \xi_m)$. Finally, (iii) the proper 1D or 2D expressions should be used for calculating the quantum conductivity.

At high temperatures $T > T^*$, in the 2D Heisenberg regime, the combination of the expressions for the 2D spin correlation length with the quantum resistance gives a linear temperature dependence of the resistivity. This result is in agreement with a well-known linear $\rho(T)$ behavior at high temperatures.

At intermediate temperatures $T_{\mathrm{MI}} < T < T^*$, in the 1D striped regime, inelastic neutron scattering experiments show evidence of the existence of dynamic stripes, and the observation of the 1D features in the transport properties should therefore not be limited to the Cu-O chain-direction only. Moreover, although the 1D stripes are dynamic, no averaging of the transport properties will occur, since, even for dynamic stripes, the charge will automatically follow the most conducting paths, i.e., stripes, even if they are moving fast. So, in transport experiments the magnetic correlation length $\xi_{m\,1\mathrm{D}}$ of a dynamic insulating AF interstripe domain permanently imposes the constraint $L_\phi \sim \xi_{m\,1\mathrm{D}}$ on metallic stripes, thus providing a persistent 1D character of the charge transport in underdoped cuprates. Inserting this inelastic length into the expression for 1D quantum conductivity yields an S-shaped $\rho(T)$ that perfectly describes the resistivity data obtained on the even-chain spin-ladder compounds $Sr_{2.5}Ca_{11.5}Cu_{24}O_{41}$ and $PrBa_2Cu_4O_8$. These compounds, due to their specific crystalline structure, definitely contain a 1D spin ladder, and therefore their resistivity along the ladder direction should indeed obey the expression for the 1D quantum transport.

As a next step, a convincing scaling was found between the resistivity of the 1D spin-ladder compound and a typical underdoped high-T_c material, $YBa_2Cu_4O_8$, demonstrating that the resistivity versus temperature dependences of underdoped cuprates in the pseudogap regime at $T < T^*$ and even-chain SL with a spin-gap Δ are governed by the same underlying 1D (magnetic) scattering mechanism. This magnetic origin of the scattering of the charge carriers is further confirmed by the fact that the scaling parameter Δ—the spin gap—used in the $\rho(T)$ scaling works equally well for resistivity as well as for the Knight-shift data $K_S(T)$. For the theoretical analysis of the $K_S(T)$ data we have used the expressions derived for 1D SL systems.

The $\rho(T)$ data of $YBa_2Cu_3O_x$ thin films with varying oxygen content, scaled onto one universal curve, are all well described by the expression for the 1D quantum transport at $T_{\mathrm{MI}} < T < T^*$. The values of the spin gap Δ, estimated from this fit, are in agreement with an independent determination of Δ from resistive measurements on other $YBa_2Cu_3O_x$ thin films and twinned and detwinned single crystals. Moreover, they agree with estimates of the pseudogap derived from the CuO_2 plane ^{17}O and ^{63}Cu Knight-shift measurements on aligned powders. In the 1D quantum transport model, where the inelastic length is assumed to be dominated by the magnetic correlation length, the agreement of our data with the gap determined from NMR experiments seems to be natural. This proves that our analysis, describing the transport in underdoped cuprates at $T < T^*$ by taking into account the presence of the 1D stripes, not only agrees qualitatively, but also yields values for the pseudo-spin-gap Δ that agree well with independent estimates.

At low temperatures $T < T_{\mathrm{MI}}$, the metallic behavior of the resistivity at high temperatures transforms into an insulating,

diverging, $\rho(T)$ curve that was shown to agree with a $\ln(1/T)$ law. Our normal-state resistivity and Hall effect data were analyzed by considering the possibility of the stripe formation in the CuO_2 plane. In this charge-stripe picture, dynamic, metallic stripes are thought to control the transport properties. So, within this model, one expects a strong influence on the transport properties when, for some reason, the 1D charge stripes are fragmented or/and pinned thus promoting the interstripe hopping.

These processes invoke a strong influence of the intercalating Mott insulator phase on the charge transport, yielding a 2D insulating resistivity and a finite Hall response. By inserting the temperature dependence of the inelastic length L_ϕ, of the scattering mechanisms applicable for the intercalating insulating phase, into the conductivity expression for 2D quantum transport, one can obtain the low-temperature $\ln(1/T)$ divergence of the high-field resistivity. For example, the inelastic length for electron-electron or electron-phonon scattering, $L_\phi \sim 1/T^\alpha$, combined with the expression for 2D quantum transport, gives an $\ln(1/T)$ correction to the low-temperature resistivity. This 2D weak-localization model also agrees with our finding of a constant Hall coefficient $R_H(T)$ at low temperatures.

The *main result* of this paper is the demonstration of a very successful application of the Moshchalkov's 1D transport model[4] [Eq. (6)] to describe a universal superlinear resistivity $\rho(T)$ in the underdoped cuprates. The analysis of the universal scaling behavior of the transport properties and the Knight-shift data have also revealed that the 1D metallic stripes in high T_c's behave as dynamic even-leg spin ladders (also see Refs. 51), and therefore *the pseudogap seen at* $T < T^*$ *is just the spin gap in these ladders*. Disorder effects result in the fragmentation of stripes and in their pinning, thus forcing the charge carriers to hop from one pinned fragment of charge carriers to another via an insulating AF domain. This interstripe hopping leads to the recovery of the 2D character of the transport properties with the $\Delta\rho(T) \sim \ln(1/T)$ insulating behavior corresponding to weak localization effects in the 2D regime.

ACKNOWLEDGMENTS

The Belgian IUAP, the Flemish GOA, and FWO programmes supported this work. J.V. is a postdoctoral fellow of the FWO-Vlaanderen.

[1] J. G. Bednorz and K. A. Müller, Z. Phys. B: Condens. Matter **64**, 188 (1986).
[2] J. Vanacken, Physica B **294**–**295**, 347 (2001).
[3] V. V. Moshchalkov, Solid State Commun. **86**, 715 (1993).
[4] V. V. Moshchalkov, cond-mat/9802281 (unpublished).
[5] V. V. Moshchalkov, L. Trappeniers, and J. Vanacken, Europhys. Lett. **46**, 75 (1999).
[6] V. V. Moshchalkov, L. Trappeniers, and J. Vanacken, Physica C **318**, 361 (1999).
[7] V. V. Moshchalkov, L. Trappeniers, and J. Vanacken, J. Low Temp. Phys. **117**, 1283 (1999).
[8] V. V. Moshchalkov and V. A. Ivanov, cond-mat/9912091 (unpublished).
[9] P. W. Anderson, J. Phys. (Paris) **8**, 10 083 (1996).
[10] E. Dagotto and T. M. Rice, Science **271**, 618 (1996).
[11] V. J. Emery, S. A. Kivelson, and O. Zachar, Phys. Rev. B **56**, 6120 (1997).
[12] J. M. Tranquada, Phys. Rev. Lett. **78**, 338 (1997).
[13] H. A. Mook, P. Dai, F. Dogan, and R. D. Hunt, Nature (London) **404**, 729 (2000).
[14] V. J. Emery, S. A. Kivelson, and O. Zachar, Phys. Rev. B **56**, 6120 (1997).
[15] V. J. Emery, S. A. Kivelson, and J. M. Tranquada, Proc. Natl. Acad. Sci. U.S.A. **96**, 8814 (1999); cond-mat/9907228 (unpublished).
[16] A. A. Abrikosov, *Fundamentals of the Theory of Metals* (North-Holland, Amsterdam, 1988).
[17] P. Hasenfratz and F. Niedermayer, Phys. Lett. B **268**, 231 (1991).
[18] D. Reefman, Ph.D. thesis, Rijksuniversiteit Leiden, 1993
[19] M. Greven, R. J. Birgenau, and U.-J. Wiese, Phys. Rev. Lett. **77**, 1865 (1996).
[20] T. Nagata, M. Uehara, J. Goto, N. Komiya, J. Akimitsu, N. Motoyama, H. Eisaki, S. Uchida, H. Takahashi, T. Nakanishi, and N. Mori, Physica C **282–287**, 153 (1997).
[21] M. Takano, M. Azuma, Y. Fujishiro, M. Nohara, H. Takagi, M. Fujiwara, H. Yasuoka, S. Ohsugi, Y. Kitaoka, and R. S. Eccleston, Physica C **282–287**, 149 (1997).
[22] S. Horii, U. Mitztani, H. Ikuta, Y. Yamada, J. H. Ye, A. Matsishita, N. E. Hussey, T. Takagi, and I. Hirabayashi, Phys. Rev. B **61**, 6327 (2000).
[23] J. Karpinski, E. Kaldis, E. Jilek, S. Rusiecki, and B. Bucher, Nature (London) **336**, 660 (1988).
[24] R. Gagnon, Ch. Lupien, and L. Taillefer, Phys. Rev. B **50**, 3458 (1994).
[25] T. A. Friedmann, M. W. Rabin, J. Giapintzakis, J. P. Rice, and D. M. Ginsberg, Phys. Rev. B **42**, 6217 (1990).
[26] B. Bucher and P. Wachter, Phys. Rev. B **51**, 3309 (1995).
[27] J. L. Cohn and J. Karpinski, cond-mat/9810152 (unpublished).
[28] R. C. Yu, M. B. Salamon, J. P. Lu, and W. C. Lee, Phys. Rev. Lett. **69**, 1431 (1992).
[29] N. L. Wang, S. Tajima, A. I. Rykov, and K. Tomimoto, Phys. Rev. B **57**, R11 081 (1998).
[30] S. Tajima, R. Hauff, W.-J. Jang, A. Rykov, Y. Sato, and I. Terasaki, J. Low Temp. Phys. **105**, 743 (1996).
[31] J. M. Tarascon, P. Barboux, P. F. Miceli, L. H. Greene, and G. W. Hull, Phys. Lett. B **37**, 7458 (1988).
[32] G. Xiao, M. Z. Cieplak, D. Musser, A. Gavrin, F. H. Streitz, C. L. Chien, J. J. Rhyne, and J. A. Gotaas, Nature (London) **332**, 238 (1988).
[33] P. Dai, H. A. Mook, and F. Dogan, Phys. Rev. Lett. **80**, 1738 (1998).
[34] Y.-J. Kao, Q. Si, and K. Levin, cond-mat/9908302 (unpublished).

[35] M. Arai, T. Nishijima, Y. Endoh, T. Egami, S. Tajima, K. Tomimoto, Y. Shiohara, M. Takahashi, A. Garret, and S. M. Bennington, Phys. Rev. Lett. **83**, 608 (1999).

[36] B. Bucher, P. Steiner, and P. Wachter, Physica B **199-200**, 268 (1994).

[37] M. Troyer, H. Tsunetsugu, and D. Würtz, Phys. Rev. B **50**, 13 515 (1994).

[38] B. Wuyts, V. V. Moshchalkov, and Y. Bruynseraede, Phys. Rev. B **53**, 9418 (1996).

[39] Y. Ando, G. S. Boebinger, A. Passner, N. L. Wang, C. Geibel, and F. Steglich, Phys. Rev. Lett. **77**, 2065 (1996); Y. Ando, G. S. Boebinger, A. Passner, N. L. Wang, C. Geibel, F. Steglich, I. E. Trofimov, and F. F. Balakirev, Phys. Rev. B **56**, R8530 (1997); Y. Ando, G. S. Boebinger, A. Passner, N. L. Wang, C. Geibel, F. Steglich, T. Kimura, M. Okuya, J. Shimoyama, K. Kishio, K. Tamasaku, N. Ichikawa, and S. Uchida, Physica C **282–287**, 240 (1997); Y. Ando, G. S. Boebinger, A. Passner, T. Kimura, and K. Kishio, Phys. Rev. Lett. **75**, 4662 (1995); Y. Ando, G. S. Boebinger, A. Passner, R. J. Cava, T. Kimura, J. Shimoyama, and K. Kishio (unpublished); Y. Ando, G. S. Boebinger, A. Passner, K. Tamasaku, N. Ichikawa, S. Uchida, M. Okuya, T. Kimura, J. Shimoyama, and K. Kishio, J. Low Temp. Phys. **105**, 867 (1996); G. S. Boebinger, Y. Ando, A. Passner, T. Kimura, M. Okuya, J. Shimoyama, K. Kishio, K. Tamasaku, N. Ichikawa, and S. Uchida, Phys. Rev. Lett. **77**, 5417 (1996).

[40] T. Timusk and B. Statt, Rep. Prog. Phys. **62**, 61 (1999).

[41] T. Ito, K. Takenaka, and S. Uchida, Phys. Rev. Lett. **70**, 3995 (1993).

[42] M. Takigawa, A. P. Reyes, P. C. Hammel, J. D. Thompson, R. H. Heffner, Z. Fisk, and K. C. Ott, Phys. Rev. B **43**, 247 (1991).

[43] J. A. Martindale and P. C. Hammel, Philos. Mag. B **74**, 573 (1996).

[44] D. Mihailovic, V. V. Kabanov, K. Zagar, and J. Demsar, Phys. Rev. B **60**, R6995 (1999).

[45] H. Alloul, P. Mendels, G. Collin, and P. Monod, Phys. Rev. Lett. **61**, 746 (1988); H. Alloul, T. Ohno, and P. Mendels *ibid.* **63**, 1700 (1989).

[46] Z. Hao, B. R. Zhao, B. Y. Zhu, Z. X. Zhao, J. Vanacken, and V. V. Moshchalkov (unpublished).

[47] S.-W. Cheong, G. Aeppli, T. E. Mason, H. Mook, S. M. Hayden, P. C. Canfield, Z. Fisk, K. N. Clausen, and J. L. Martinez, Phys. Rev. Lett. **67**, 1791 (1991).

[48] T. Noda, H. Eisaki, and S. Uchida, Science **286**, 265 (1999).

[49] N. Ichikaàwa, S. Uchida, J. M. Tranquada, T. Niemoller, P. M. Gehring, S. H. Lee, and J. R. Schneider, cond-mat/9910037 (unpublished).

[50] S. A. Kivelson, E. Fradkin, and V. J. Emery, Nature (London) **393**, 550 (1998).

[51] R. S. Markiewicz, Phys. Rev. B **62**, 1252 (2000).